Splitting of the interband absorption edge in Au

M. Guerrisi and R. Rosei*
Istituto di Fisica, Università di Roma, Roma, Italy

P. Winsemius†
Kamerlingh Onnes Laboratorium, University of Leiden, The Netherlands
(Received 26 November 1974)

Very accurate ellipsometric measurements were made on very pure bulk samples of Au at room temperature in the 1.0–3.5-eV energy region. A model calculation has been developed for d bands to Fermi-surface transitions occurring near the X point in the Brillouin zone and it is shown that for topological reasons the line shape of the imaginary part of the dielectric constant ϵ_2 is considerably different from what has been calculated for L transitions. Using this model to fit our experimental data it has been possible to show that the absorption edge in Au is "split" into two separate contributions. The onset of X transitions has been located at 1.94 eV while the onset of the L transitions has been confirmed at 2.45 eV in excellent agreement with previous determinations.

I. INTRODUCTION

The characteristic shape of the interband transition edge of gold has been the subject of considerable interest and speculation in recent years. While it is widely recognized that the steep rise of ϵ_2 at about 2.5 eV is originating from d bands to Fermi-surface transitions near L, much more puzzling is the origin of a long nearly exponential tail which extends well below 2 eV.

Indeed, in their pioneering paper[1] Cooper, Ehrenreich, and Philipp showed, using a model calculation, that the expected line shape for the joint density of states at zero temperature should behave like a square-root singularity (roughly like an M_0 critical point).

Several authors[2,3] have been able to fit their experimental data with the expected line shape in a limited energy region. Even taking into account the expected temperature broadening of the edge due to the Fermi-distribution smearing out, it is not possible to explain the magnitude and extention of the low-energy tail. Various mechanisms were proposed: Nilsson *et al.*[2] speculated that deformation of electronic bands due to lattice defects was to be held responsible, or alternatively the lifetime broadening of the absorption edge; Thèye[3] also found an irreducible tail in her very careful measurements on thin films and invoked an Auger-type broadening of the edge.

Lately, the belief that the tailing of the absorption edge is largely due to genuine interband transitions has been prevailing.[4–6] As a matter of fact, Christensen and Seraphin[4] showed that the change of slope at 2.2 eV follows directly from the band calculation, the first transition occurring from band 5 to band 6 (at E_F) near X.

Szczepanek and Glosser[5] find structure starting at about 1.8 eV in the tetragonal spectra of their piezomodulation experiment and assign it to interband transitions near X.

Despite the growing evidence, a few interrogatives remain on the role of the X transitions. Even if it is acknowledged that they may have much weaker dipole matrix element, it is not clear why they present a smooth increase instead of a steep edge as L transitions do. Also puzzling is their failure to appear in thermomodulation experiments,[7–9] since it is recognized that transitions ending at the Fermi surface give an important contribution in these spectra.

In Sec. II we present new very accurate experimental data of the imaginary part of the dielectric function ϵ_2 of gold in the interband onset region.

In Sec. III we give the derivation of the line shape for the X transitions extending a technique already successfully used to fit thermomodulation data[10,11] and the absorption edge of Ag.[12] It is shown that indeed, owing to the topology of the constant-energy surfaces (CES) and of the constant-energy-difference surfaces (CEDS) in k space, the theory predicts a smoothly sloping edge in contrast with the steep edge characteristic of L transitions.

Section IV shows how the experimental data can be fitted in the onset region summing the contributions for both X and L transitions. Finally, in Sec. V the reasons for the failure of the X transitions to appear in thermomodulation data are elucidated and suggestions are given for designing an experiment which would bring out their contribution.

II. EXPERIMENTAL

A. Experimental setup

Using the method of Beattie,[13] the optical properties of Au were measured between 1.0 and 3.5 eV at room temperature (angle of incidence $\approx 69°$). During all measurements vacuum in the cold-finger cryostat was of the order of 10^{-7} Torr or better.

Experimental conditions in this photon-energy

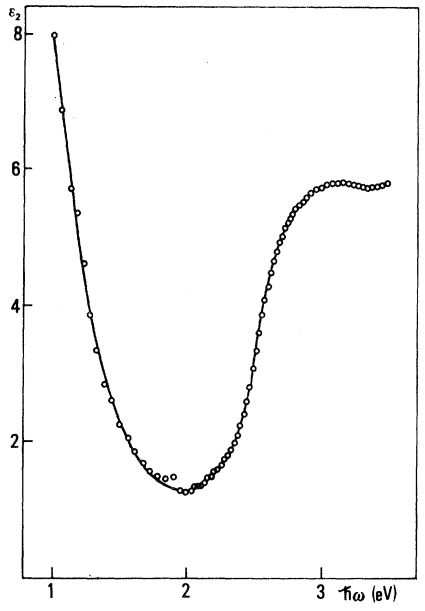

FIG. 1. Imaginary part of the dielectric constant for Au.

interval are particularly favorable. The signal-to-noise ratio of light source plus detector is high, whereas the degree of polarization of the light emitted by the tungsten ribbon filament lamp is negligible.[14] The angular polarized field of the double Glan-Taylor polarizers is almost symmetrical at 14°, thus facilitating the alignment of the polarizers. Also, using a servo system[15] the accuracy and reproducibility of the angular setting of the polarizers is better than 1′. Under these conditions a calculation of the random error[6] yields $\Delta\epsilon_1/\epsilon_1$ between 0.5 and 1.5% and $\Delta\epsilon_2/\epsilon_2 \approx 0.3\%$ — or translating into absolute values — $|\Delta\epsilon_2| \lesssim 0.02$. An estimate of the systematic error is much harder (see also next paragraph). An indication may be obtained from the reproducibility of measurements upon complete readjustment of all optical components that yielded $|\Delta\epsilon_2| < 0.05$.

By appropriate choice of the monochromator slit widths and through the use of a computer calibration of the dispersion[6,16] the systematic error in the measurement of the photon energy is always less than 0.005 eV. The random error is determined by the accuracy of the reading of the monochromator setting and is estimated to be ± 0.002 eV.

B. Specimen preparation

A polycrystalline Au sample (purity, 99.999%; average grain diameter 1.5 mm) was grown by standard vacuum techniques and subsequently cut and planed into its required shape (diameter, 27 mm; thickness, 3.5 mm) by spark erosion. Initial polishing was by etch attack[17] using an abrasive slurry made up of Al_2O_3 powder (final stage 0.05 μm) and a 10-wt% CrO_3 solution. The specimen then was electropolished on a rotating wheel machine similar in design to the acid polishing machine by Dyer.[18] Best results were obtained using an electrolyte consisting of 9.6-g $Na_2S_2O_3$, 4.2-g NH_4CNS, 5-ml H_2SO_4 (96%), 5-ml HF (40%), 285-ml butylcellosolve, and 55-ml deionized H_2O; the current density was 3.5 mA/cm^2. The surfaces thus obtained are shiny, flat except for a rounding at the edges, and did not show any relief structure that can arise due to preferential attack of some crystallites. Polishing was continued until all traces of mechanical polishing were removed as was confirmed by x-ray diffraction tests.

Directly after polishing, the sample was mounted in the specimen holder and the vacuum chamber was pumped down. At all further stages of the experiment the vacuum was of the order of 10^{-7} Torr or better. Prior to the measurements the sample was annealed at temperatures of 700 K or higher for at least 4 h. This high-temperature treatment gives rise to some surface roughness caused by thermal etching. However, as shown elsewhere[19] the optical spectra obtained on this sample give no indication of internal strain such as is often found in films and mechanically polished samples. Also, in a large number of additional measurements (after repolishing and/or extensive annealing), the ϵ_2 data were found to be highly reproducible for photon energies between 1.0 and 3.5 eV. Figure 1 presents the results of ϵ_2 measurements.

III. X-TRANSITIONS JOINT DENSITY OF STATES

The joint density of states (JDOS) for any couple

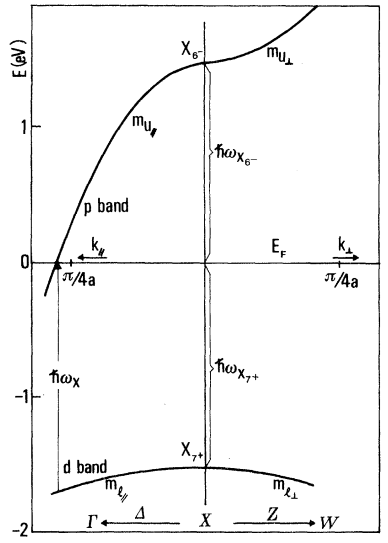

FIG. 2. Detail of the band structure near X for Au.

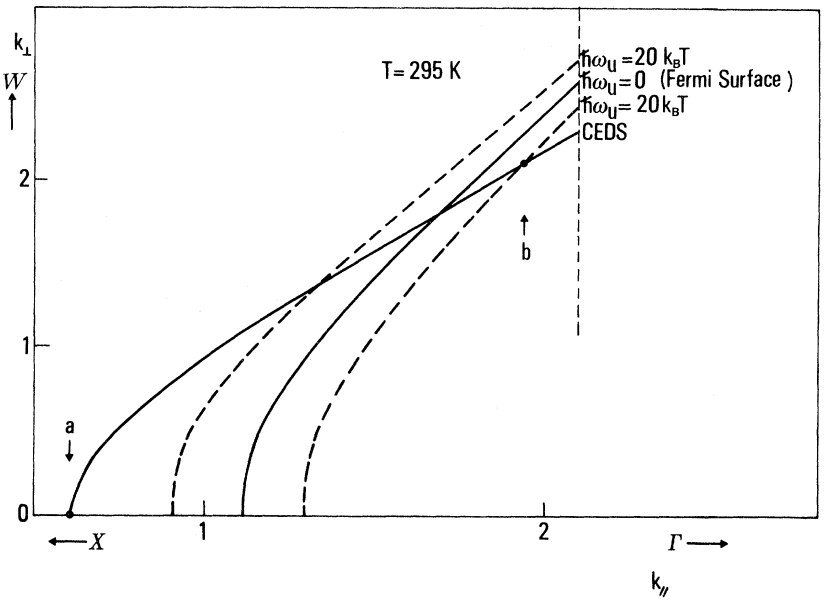

FIG. 3. Detail of the Fermi surface near X showing (100) cross section of a typical CEDS and constant final-energy surfaces. $k_\perp$ and $k_\parallel$ are in units of $\pi/4a$.

of bands can be obtained integrating the energy distribution of the joint density of states (EDJDOS).[20,21]

When the initial or the final band crosses the Fermi energy, this procedure allows the calculation of the effect brought about by the Pauli exclusion principle in a very straightforward manner and also the temperature smearing of the absorption edge is automatically calculated.[10]

Figure 2 shows a detail of the band structure of gold near X. $\hbar\omega_X$ marks the onset of interband transitions in this region. Assuming the energy bands depend quadratically on the distance from X and assuming rotational symmetry around Δ we may write the equation for a constant-energy surface of the upper (u) band[22]:

$$\hbar\omega_u = \hbar\omega_{X_6^-} + \frac{\hbar^2 k_\perp^2}{2m_{u\perp}} - \frac{\hbar^2 k_\parallel^2}{2m_{u\parallel}} = E \ . \tag{1}$$

Similarly the equation for a constant-energy surface of the lower (l) band is given by

$$\hbar\omega_l = -\hbar\omega_{X_{7^+}} - \frac{\hbar^2}{2m_{l\perp}} k_\perp^2 - \frac{\hbar^2}{2m_{l\parallel}} k_\parallel^2 = E - \hbar\omega \ . \tag{2}$$

The transitions between these two bands at photon energy $\hbar\omega$ are restricted to the surface of constant interband energy

$$\Omega_{lu}(\vec{k}) = \hbar\omega_u - \hbar\omega_l - \hbar\omega = 0 \ . \tag{3}$$

The EDJDOS for this pair of bands can now easily be calculated following the procedure outlined in Ref. 10. One obtains

$$\mathfrak{D}_{l\to u}(E, \hbar\omega) = (8\pi^2\hbar^2)^{-1} \mathfrak{F}_{l\to u} k_\parallel^{-1} \ , \tag{4}$$

where $\mathfrak{F}_{l\to u}$ is given by

$$\mathfrak{F}_{l\to u} = \left(\frac{m_{l\perp} m_{u\parallel} + m_{l\parallel} m_{u\perp}}{m_{l\perp} m_{l\parallel} m_{u\perp} m_{u\parallel}} \right)^{-1/2} \tag{5}$$

and

$$k_\parallel = \left(\hbar\omega - \hbar\omega_{X_{7^+}} + \frac{\hbar^2}{2m_{l\perp}} (\hbar\omega_{X_{6^-}} - E) - \frac{\hbar^2}{2m_{u\perp}} E \right)^{1/2} . \tag{6}$$

For the joint density of states we finally obtain:

$$\mathfrak{J}_{l\to u}(\hbar\omega, T) = \int_{E_{\min}}^{E_{\max}} \mathfrak{D}_{l\to u}(E, \hbar\omega)[1 - f(E, T)]\, dE \ , \tag{7}$$

where the factor in square brackets gives the probability that a state with energy E in the upper band is empty.

Referring to Fig. 3, it can be seen that the upper limit of integration is given by

$$E_{\max} = \hbar\omega_{X_{6^-}} + (\hbar\omega_{X_{7^+}} + \hbar\omega_{X_{6^-}} - \hbar\omega)\, m_{u\parallel}/(m_{l\parallel} - m_{u\parallel}) \ . \tag{8}$$

while at each temperature the lower limit of integration can be safely assumed to be about $-20\ k_B T$ for calculational purposes. Figure 4 reports the shape of the JDOS obtained for zero, room temperature and 600 K.

It is very important to note that even at 0 K the X transitions do not present a sharp edge but only a gently sloping absorption. Their behavior is therefore quite different from that presented by L transitions.[10]

This difference can be traced in the different topology of CES and CEDS at X and L, respectively, as will be explained in the following.

In order to understand physically this behavior it is convenient to follow the "path" of the function

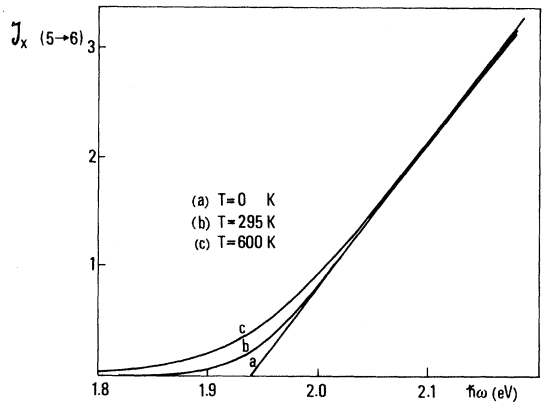

FIG. 4. Joint density of states of Au due to band-5–band-6 transitions near X calculated at different temperatures.

$\mathfrak{D}_{l\to u}(E, \hbar\omega)$ for different photon energies $\hbar\omega$.

Figure 5 shows the CEDS corresponding to six different interband photon energies together with the Fermi surface, while Fig. 6 gives the EDJDOS calculated at the same energies. In other words each curve in Fig. 6 shows how the density of interband transitions is distributed on the corresponding CEDS of Fig. 5. The boxlike functions in Fig. 6

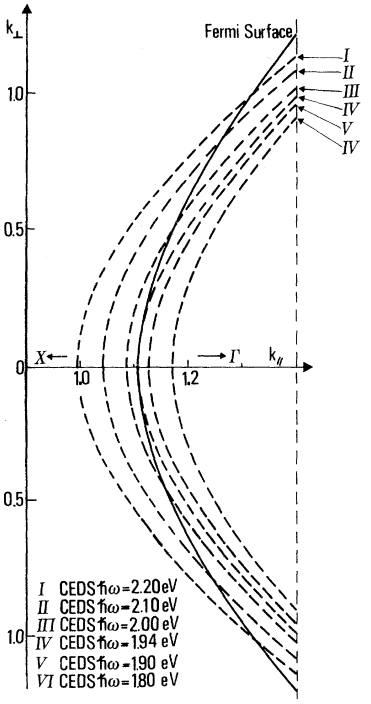

FIG. 5. Cross section of the Fermi surface and of CEDS in the region near X on a plane containing the X-Γ direction. $k_\perp$ and $k_\parallel$ are in units of $\pi/4a$.

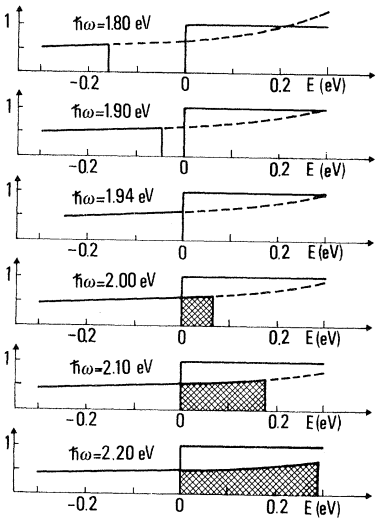

FIG. 6. Absorption mechanism for band-5–band-6 transitions near X. The EDJDOS (E) is reported for several photon energies. The boxlike function gives in each case the probability that the final state is empty at zero temperature. The integrand in Eq. (7) is given by the product of the two curves. The absorption is given in each case by the hatched areas.

represent the probability $P(E) = 1 - f(E, 0)$ that the final state is empty at zero temperature.

It is important to note that the singularity exhibited by the EDJDOS is in this case steplike, [23] while the corresponding EDJDOS for L transitions presents an inverse square-root singularity. The different behavior can be easily understood when it is realized that for L transitions the CEDS corresponding to the onset is tangent to the Fermi surface along a circle (the neck of the Fermi surface) thus giving rise to an infinite density of possible transitions with final energy in an interval E_{FS}, $E_{FS} + dE$. At X, the tangency is limited to a point and the discontinuity of the EDJDOS should therefore be finite.

Following now the "path" of the EDJDOS on increasing the photon energies, it is easily understood that above the edge, obtained for $\hbar\omega = \hbar\omega_X = 1.94$ eV, the absorption (which is proportional to the shaded areas) increases approximately linearly with photon energies.

IV. FITTING PROCEDURE

In Sec. III we obtained the JDOS for transitions near X. The procedure for obtaining the JDOS for transitions at L has been presented in a number of papers [10, 12] and will not be repeated here.

In the constant matrix element approximation the JDOS can be easily related to the imaginary part of the dielectric function. In the following it will be assumed that the dipole element for X transi-

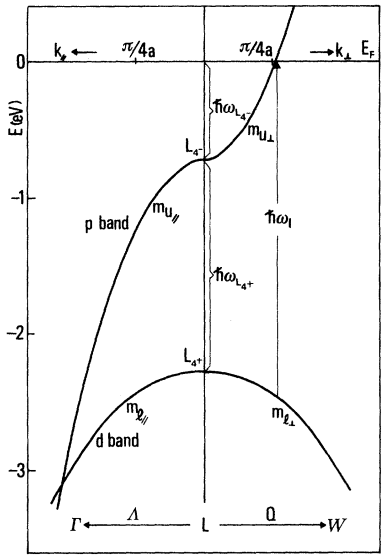

FIG. 7. Detail of the band structure near L for Au.

tions $P_X(l \to u)$ is approximately constant in a small region near X [of the order of $(\pi/10a)^3$] and the same is true for the dipole matrix element for L transitions $P_L(l \to u)$ in a small region near L.

Assuming that in the region around and just above the onset no other interband transition contributes, we can write

$$\epsilon_2(\hbar\omega, T) = \frac{8\pi^2 e^2 \hbar^4}{3m^2(\hbar\omega)^2} \times [\,|P_X(l \to u)|^2 \mathcal{J}_X(\hbar\omega, T) + |P_L(l \to u)|^2 \times \mathcal{J}_L(\hbar\omega, T)\,] . \quad (9)$$

Using this analytic expression for ϵ_2 we tried to fit our experimental data to about 2.7 eV. Only limited regions in K space around X and around L are involved in our model when the fitting is extended a few tenths of an eV above the absorption edge. It should be remembered however that although occurring in different regions of the Brillouin zone (BZ): we are dealing in both cases with band-5–band-6 transitions. The danger of counting transitions twice and of a breakdown of our approximations may therefore arise at higher photon energies.

The energy gaps shown in Figs. 2 and 7 were used as fitting parameters as well as the "strength" of the two transitions defined, respectively, as

$$S_X = \mathcal{F}_X |P_X(l \to u)|^2 , \quad S_L = \mathcal{F}_L |P_L(l \to u)|^2 . \quad (10)$$

The experimental data were first corrected by subtracting the background absorption (which has been supposed to be Drude-like).

The fit is shown in Fig. 8. The result we obtained is fairly good also using the nominal temperature 295 K but a much better one can be obtained using an effective temperature $T = 600$ K (Fig. 8, curve a). Curves b and c of Fig. 8 give, respectively, the contribution of X and L transitions to the total absorption.

The parameters used for the fitting were

$$\hbar\omega_{L_4^+} = 1.560 \text{ eV} , \quad \hbar\omega_{X_7^+} = 1.770 \text{ eV} ,$$
$$|P_X/P_L|^2 = 0.370 .$$

The other parameters requested by the theory, e.g., the optical masses and the gaps $\hbar\omega_{X_6^-}$ and $\hbar\omega_{L_4^-}$ were taken from Ref. 4.

It should be noted that this fitting allows for the first time a direct determination of the k dependence of the optical dipole matrix element and shows that the usual approximation of setting it constant throughout the whole BZ involves large errors.

We have used our model for fitting also other experimental data taken from Ref. 3. It is particularly interesting to compare the results since Thèye's data were taken on thin films while our data were taken on bulk samples. We obtained an excellent fit using the parameters

$$\hbar\omega_{L_4^+} = 1.565 \text{ eV} , \quad \hbar\omega_{X_7^+} = 1.650 \text{ eV} ,$$
$$|P_X/P_L|^2 = 0.321 ,$$

and an effective temperature T of 700 K.

It is striking that while the L gap does not change

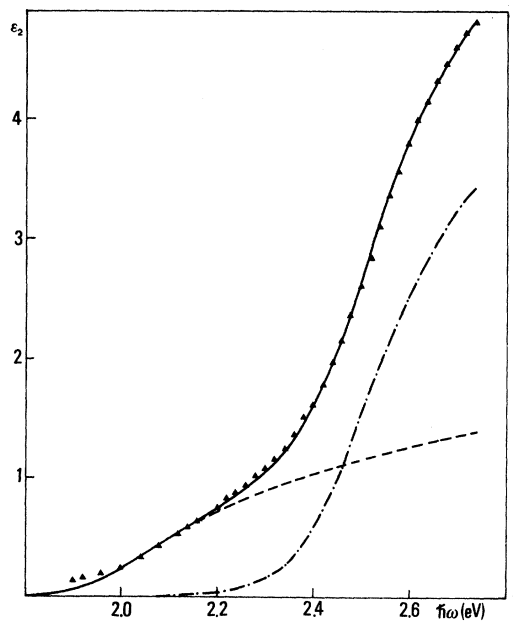

FIG. 8. Imaginary part of the dielectric constant for Au: solid triangles, experimental; dashed line, X-transitions contribution; dot-dashed line, L-transitions contribution; solid line, total theoretical.

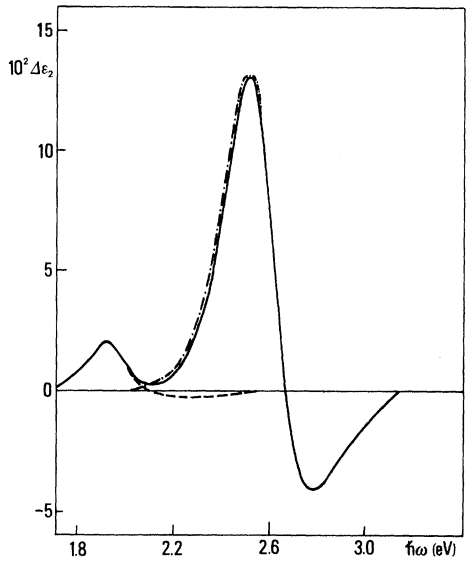

FIG. 9. Theoretical thermomodulation spectra of $\Delta\epsilon_2$ for Au: dashed line, X-transitions contribution; dot-dashed line, L-transitions contribution; solid line, total theoretical. The same effective temperature was used ($T = 600$ K), which fits the static data.

noticeably, the X gap differs in the two measurements by about 0.12 eV. Even taking into account the uncertainty brought about by the subtraction of the Drude term, still it must be concluded that even the most careful measurements on thin films may lead to errors in the determination of optical gaps.

While it is not certain why also for fitting bulk data it had to be used an effective temperature a factor of 2 higher than the actual one, it is also evident that thin film samples must be somewhat more disordered thus making the Fermi distribution more smeared out.

V. THERMODERIVATIVE LINE SHAPE

From the analytic expression of the EDJDOS it is very simple to obtain the contribution to the derivative spectra due to the Fermi-surface smearing out.

In Ref. 10 it is shown that such contribution for d bands to Fermi surface transitions is given by

$$\Delta\epsilon_2 = \frac{C}{(\hbar\omega)^2}\left[\int_{E_{\min}}^{E_{\max}} \mathfrak{D}(E, \hbar\omega)\left(-\frac{\partial}{\partial T} f(E, T)\right) dE\right]\Delta T \tag{11}$$

where C is a constant proportional to the dipole matrix element of the transition and $f(E, T)$ is the Fermi distribution function.

It is therefore straightforward now to "predict" the line shape of thermomodulation spectra if it is assumed that also X transitions have a fairly small deformation potential.[24] Figure 9 shows the expected compound line shape of $\Delta\epsilon_2$ in the interband onset region together with the contributions expected from transitions at X and L, respectively.

The different topology in k space is reflected also in the thermoderivative behavior. The X transitions, in fact, show a much smaller negative dip which stretches as a long tail for several tens of an eV.

The $\Delta\epsilon_2$ theoretical spectra have also been Kramers-Krönig analyzed and the "predicted" spectra of $\Delta R/R$ have been obtained through the formula[25].

$$\Delta R/R = A(\epsilon_1, \epsilon_2)\Delta\epsilon_1 + B(\epsilon_1, \epsilon_2)\Delta\epsilon_2 . \tag{12}$$

The results are shown in Fig. 10 which shows the contributions originating from the X and L transitions. The parameters used were those determined from fitting our experimental data. The amplitude of the thermal wave ΔT[8] was taken 1 K.

It can be noted that in the thermoreflectance spectrum the X contribution is even more depressed since the coefficients A and B in Eq. (12) tend to become much smaller in the infrared (see insert in Fig. 10). The peak modulation of the X transitions contribution to $\Delta R/R$ is about a factor of 40 smaller than the contribution due to the L transitions. It should also be considered that in thermoderivative experimental spectra the contribution of the intraband transitions modulation is present in the form of a background slowly rising toward the infrared.[8] It is therefore not surprising that the X transition contribution to thermomod-

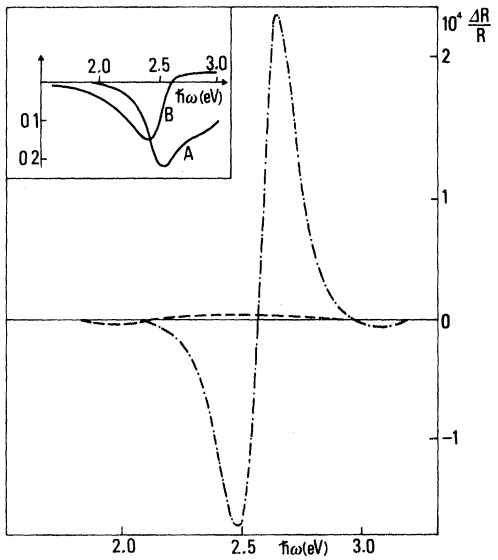

FIG. 10. Theoretical thermomodulation spectra of $\Delta R/R$ for Au: dashed line, X-transitions contribution; dot-dashed line, L-transitions contribution. The insert shows the energy dependence of the A and B coefficients of Eq. (12).

ulation spectra of gold has never been noted before.

It is suggested that a careful thermomodulation experiment, performed on bulk samples at very low temperature may confirm our findings and also help to resolve the question of the exact position of the onset of the X transitions.

---

*Gruppo Nazionale di Struttura della Materia del Consiglio Nazionale delle Ricerche.

†Part of the research program of the Foundation F.O.M. supported by Z.W.O. and T.N.O. (Metaalinstuut).

[1]B. R. Cooper, H. Ehrenreich, and H. R. Philipp, Phys. Rev. 138, A494 (1965).

[2]P. O. Nilsson, A. Persson, and H. Norden, Ark. Fysik. 35, 165 (1967).

[3]M. L. Thèye, Phys. Rev. B 2, 3060 (1970).

[4]N. E. Christensen and B. O. Seraphin, Phys. Rev. B 4, 3321 (1972).

[5]P. S. Szezepanek and R. Glosser, University of Maryland, Technical Report, 1973 (unpublished); and Solid State Commun. 15, 1425 (1974).

[6]P. Winsemius, Ph. D. thesis (University of Leiden, 1973) (unpublished), available upon request.

[7]W. J. Scouler, Phys. Rev. Lett. 18, 455 (1967).

[8]R. Rosei and D. W. Lynch, Phys. Rev. B 5, 3883 (1972).

[9]R. Rosei, F. Antonangeli, and U. M. Grassano, Surf. Sci. 37, 689 (1973).

[10]R. Rosei, Phys. Rev. B 10, 474 (1974).

[11]R. Rosei, C. H. Culp, and J. H. Weaver, Phys. Rev. B 10, 484 (1974).

[12]F. Antonangeli, E. Colavita, R. Rosei, and S. E. Salusti, Nuovo Cimento B 24, 121 (1974).

[13]J. R. Beattie, Philos. Mag. 46, 235 (1955).

[14]H. P. Lengkeek and P. Winsemius (unpublished).

[15]J. A. G. Verkuyl, H. P. Lengkeek, and P. Winsemius, J. Phys. E 6, 322 (1973).

[16]R. E. Fryer, Appl. Opt. 6, 275 (1967).

[17]L. E. Samuel, *Metallographic Polishing by Mechanical Methods*, 2nd ed. (Pitman, Melbourne, 1971), p. 145.

[18]L. D. Dyer, Rev. Sci. Instrum. 34, 114 (1963).

[19]P. Winsemius, H. P. Lengkeed and F. F. Van Kampen (unpublished).

[20]R. Y. Koyama and N. V. Smith, Phys. Rev. B 2, 3049 (1970).

[21]N. V. Smith, Phys. Rev. B 3, 1862 (1971).

[22]This model is similar in spirit to the model developed by I. Lindau and L. Wallden [Phys. Scrip. 3, 77 (1971)] for interpreting their photoemission data on Cu.

[23]E. O. Kane, Phys. Rev. 175, 1039 (1968).

[24]This assumption is somewhat shaky even if no direct measurement of the deformation potential of this transition still exists in view of the large difference we have found in the positions of the onset of thin film compared to bulk samples. The statement could be made rigorous calculating the contribution at very low temperature.

[25]M. Cardona, *Solid State Physics*, edited by F. Seitz, D. Turnbull, and E. Eherenreich (Academic, New York, 1969), Suppl. 11.